Author's Accepted Manuscript

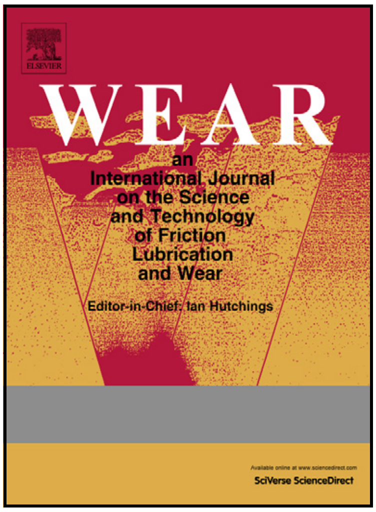

www.elsevier.com/locate/wear

Indentation and Scratch Testing of DLC-Zr coatings on Ultrafine-Grained Titanium Processed by High-Pressure Torsion

Chuan Ting Wang, Ana Escudeiro, Tomas Polcar, Albano Cavaleiro, Robert J.K. Wood, Nong Gao, Terence G. Langdon

PII: S0043-1648(12)00461-9
DOI: http://dx.doi.org/10.1016/j.wear.2012.12.033
Reference: WEA100478

To appear in: *Wear*

Received date: 17 October 2012
Revised date: 18 December 2012
Accepted date: 20 December 2012

Cite this article as: Chuan Ting Wang, Ana Escudeiro, Tomas Polcar, Albano Cavaleiro, Robert J.K. Wood, Nong Gao and Terence G. Langdon, Indentation and Scratch Testing of DLC-Zr coatings on Ultrafine-Grained Titanium Processed by High-Pressure Torsion, *Wear,* http://dx.doi.org/10.1016/j.wear.2012.12.033

Indentation and Scratch Testing of DLC-Zr coatings on Ultrafine-Grained Titanium Processed by High-Pressure Torsion

Chuan Ting Wang [a,b], Ana Escudeiro[c], Tomas Polcar[a], Albano Cavaleiro[c], Robert J.K. Wood[a], Nong Gao [b,*] and Terence G. Langdon [b,d]

[a] National Centre for Advanced Tribology at Southampton, Faculty of Engineering and the Environment, University of Southampton, Southampton SO17 1BJ, UK
[b] Materials Research Group, Faculty of Engineering and the Environment, University of Southampton, Southampton SO17 1BJ, UK
[c] SEG-CEMUC – Department of Mechanical Engineering, University of Coimbra, 3030-788 Coimbra, Portugal
[d] Departments of Aerospace & Mechanical Engineering and Materials Science, University of Southern California, Los Angeles, CA 90089-1453, USA

Abstract

High-pressure torsion was employed to refine the microstructure of grade 2 Ti under an imposed pressure of 3.0 GPa at room temperature. The microhardness of grade 2 Ti increased from 1.82 GPa for the coarse grain state to 3.05 GPa after high-pressure torsion processing, where this value is very close to the hardness of the Ti-6Al-4V alloy. Subsequently, several diamond-like carbon (DLC) coatings with thicknesses of ~1.4 μm were deposited on as-received Ti, high-pressure torsion processed Ti and Ti-6Al-4V samples via physical vapour deposition. Both indentation and scratch tests showed a much improved adhesion of DLC-7Zr, DLC:H-7Zr and DLC-9Zr coatings with high-pressure torsion processed Ti as the substrate by comparison with the same coatings on coarse-grained Ti. The results suggest that commercial pure Ti processed by high-pressure torsion and coated with a diamond-like carbon coating provides a potential candidate material for bio-implant applications.

Keywords: High-pressure torsion, titanium, DLC-Zr coatings, adhesion, bio-implants

Corresponding author: Nong Gao (Tel: +44238 0593396; Fax: +44238 0593016; e-mail: n.gao@soton.ac.uk)

1 Introduction

Human joints might suffer from pain and functional loss due to degenerative diseases, aging and accidents. A total joint replacement is regarded as an effective procedure for treating joint diseases and fractures [1]. A technical survey reported that there is an increasing demand for new and improved implants because of a rapidly growing patient population and increasing numbers of younger patients [2]. The Ti-6Al-4V alloy was designed originally for the aerospace industry but it has been used widely for biomedical applications due to its high strength, good fatigue characteristics, bio-tolerance and excellent corrosion resistance [1]. Despite these attractive qualities, Ti-6Al-4V has significant drawbacks which limit its further capacity to be used as an orthopaedic and dental implant material. For example, the toxic Al and V ions released from Ti-6Al-4V may cause long-term health problems and adverse reactions with body tissues [3, 4]. Therefore, there is now an urgent need for exploring the potential for developing other bio-metals.

Pure titanium has excellent properties including high corrosion resistance, low electronic conductivity, a low ion-formation tendency and very good biocompatibility. All of these characteristics make it a very good candidate as an implant material. Nevertheless, pure titanium has a relatively low strength and a very poor wear resistance when it is subjected to sliding and abrasion. Thus, it is generally not suitable for use in artificial joints which seek materials with high strength and good tribological properties. Recently, pure titanium with ultra-fine grain sizes, processed through the application of severe plastic deformation (SPD), appears to offer an alternative possibility for the production of implant materials [5, 6]. In severe plastic deformation processing, a high level of straining is imposed on a metal using an extensive hydrostatic pressure and the strain is achieved without changing the overall dimensions of the material [7, 8]. Thus, a very large strain may be imposed on materials via repeated severe plastic deformation processing. The ultrafine-grained (UFG) materials produced by severe plastic deformation often possess extraordinary properties, including both high strength and toughness [9], long fatigue life [10, 11] and reasonable wear resistance [12, 13]. To date, various severe plastic deformation processing methods have been applied successfully for the production of high strength pure Ti [6, 14-17]. However, the evidence suggests that severe plastic deformation processing may lead to only a relatively minor improvement in the wear resistance of Ti [5, 18]. As an alternative approach, it appears that surface treatments or coatings may be necessary to enhance the service durability of titanium as implant components [19].

The idea of improving wear resistance of Ti alloys via surface treatment has been reported extensively. Surface engineering technologies such as thermal oxidation, ion implantation and thin coatings can significantly improve the tribological properties of Ti alloys. The high strength of coatings were favourable to maintain the low surface roughness during sliding motion, which also led to less wear loss of the polyethylene counterpart [20, 21].

In recent years, attention has moved to surface engineering of ultrafine-grained Ti. High-current-density nitrogen ion implantation was used to enhance the wear resistance of ultrafine-grained Ti and the results demonstrated the potential for forming a hard layer with good wear and corrosion resistance on the surface of ultrafine-grained Ti via ion implantation [22]. However, this method required that the samples were held at the relatively high temperature of 820 K and there is evidence this may be recrystallization of the ultrafine-grained structure of Ti when the temperature is above ~620 K [23]. It appears, therefore, that Chemical vapour deposition (CVD) and Physical vapour deposition (PVD) may be better approaches for this purpose because this permits the use of a lower processing temperature and easier control over the surface roughness. It is important to note that PVD methods such as magnetron sputtering can be controlled at room temperature leading to a much lower internal stress at the interface. For example, a thin and hard TiN coating was deposited on both coarse-grained and ultrafine-grained Ti substrates using PVD at a temperature below 420 K in a recent study [19]. The subsequent wear tests showed that the TiN coating improved the wear resistance of Ti by nearly two orders of magnitude and the ultrafine-grained Ti was a better substrate than coarse-grained Ti due to its higher strength. Therefore, a PVD coating on ultrafine-grained Ti shows significant promise for further exploration in future bio-implant applications.

Diamond-like carbon (DLC) coatings are regarded as other good candidates for the purpose of wear protection because of their excellent mechanical and tribological properties such as high hardness, good wear and corrosion resistance. Moreover, DLC coatings also have a much lower coefficient of friction (COF) which can also reduce the wear of the counter surface during sliding [24]. To date, several studies have explored DLC coatings for bio-implant use [25-27]. Despite the excellent tribological properties of DLC coatings, delamination of the coatings was a major problem which appeared to limit their application as articulating joints [25]. It is reasonable to anticipate that, once removed from the substrate, these DLC coating particles would act as a third body causing severe damage to the substrate or even severe reactions with the tissue. In order to solve these issues, studies have been reported exploring the use of new interlayers to improve the bonding of DLC coatings [28]. Doping with metallic elements, such as Cr [21, 29], Ti [30] and W [31], may also improve the adhesion and wear resistance. Recently, zirconium was used as a dopant metal to provide low-toxicity, good tribological behaviour and high corrosion resistance [32-34].

The present investigation was therefore initiated in order to explore the effect of substrate microstructure on the adhesion behaviour and scratch resistance of DLC-7Zr, DLC:H-7Zr and DLC-9Zr coatings deposited on grade 2 pure titanium substrates both with and without high-pressure torsion processing and, in addition, to make a direct comparison with deposition on a Ti-6Al-4V substrate.

2 Experimental materials and procedures

2.1 Materials and processing

The experiments were conducted using grade 2 pure titanium having a composition of 0.015 H, 0.1 C, 0.25 O, 0.03 N, 0.3 Fe and Ti for balance (wt. %) and the Ti-6Al-4V alloy with extra low interstitials. Initially, some of the grade 2 Ti samples were subjected to high-pressure torsion processing. The samples for high-pressure torsion were machined into disks with a diameter of 10 mm and thicknesses between 0.80 and 0.85 mm. During high-pressure torsion, the disk samples were held in shallow depressions on the faces of two massive anvils, a load was applied and then torsional straining was achieved through rotation of the lower anvil. In high-pressure torsion, the shear strain, γ, at different position of the disk can be estimated using the relationship [35]:

$$\gamma = \frac{2\pi NR}{h} \tag{1}$$

where N is the number of rotation revolutions, R is the distance from the centre of the disk and h is the height (or thickness) of the sample. In this study, high-pressure torsion processing was conducted using an imposed pressure of 3.0 GPa for 10 revolutions under quasi-constrained conditions in which there is some restricted outflow of material around the periphery of the disk during the processing operation [36, 37]. Additional details on the principles of high-pressure torsion processing are given in earlier reports [38-40].

Microhardness testing of the samples was performed under an indentation load of 1 kg for 15 seconds. As described earlier [19], tensile testing was conducted at room temperature after high-pressure torsion processing using an initial tensile strain rate of 1.0×10^{-2} s^{-1}. The microstructures of the materials were examined using a JEM 3010 transmission electron microscope (TEM) operating under an accelerating voltage of 200 kv. A detailed description of these analytical procedures was given in earlier reports [5, 19].

2.2 Coating Deposition and Characterization

Prior to deposition, the substrates were polished to a roughness less than 50 nm, cleaned in an ultrasonic bath in acetone, ethanol and distilled water for 15 min, and then etched using Ar^+ bombardment for 1 h at a substrate bias voltage of -650 V in order to remove all contaminants and oxides on the substrate surface. The coatings were deposited using dc dual magnetron sputtering in an Ar atmosphere (non-reactive process) and $Ar+CH_4$ (reactive process) to produce non-hydrogenated and hydrogenated coatings, respectively. Two targets were used: Titanium was used to deposit an interface layer and a graphite target was used with embedded Zr pellets to prepare functional film. Table 1 summarizes the deposition parameters. The work pressure was maintained constant for both reactive and non-reactive sputtering by adjusting the gas flow. A pulsed bias voltage of -50 V and a frequency of 250 kHz were applied. A TiN/TiCN interlayer with a varying composite gradient and a thickness of 450 nm was deposited in order to improve adhesion. The thickness of the functional coating was approximately 1 μm so that the total film thickness was of the order of ~1.4 μm. To facilitate a detailed description of the results, the coatings were denoted as DLC-XZr and DLC:H-XZr, where X represents the zirconium content.

The chemical composition was determined by electron probe microanalysis (EPMA) applying a 10 keV voltage. The coating hardness was measured by depth-sensing indentation using a Berkovich indenter and a load of 5 mN. A series of 32 indentations from two distinct areas was carried out in order to critically evaluate the hardness of the coatings. In addition, the reduced Young modulus was derived from the indentation measurements using the standard method [41]. The Young modulus was calculated using the following parameters: E_i = 1140 GPa and ν_i = 0.07 for the diamond indenter and ν = 0.3 for the coating [41].

2.3 Rockwell C Indentation and Scratch Test

The coating adhesion to the Ti substrates was evaluated using Rockwell C indentation and scratch testing where these are standard techniques commonly used to quantify the interfacial strength of coating-substrate systems. During the Rockwell C indentation test, a cone-shaped diamond 120° tip (200 µm in radius) was indented perpendicularly onto the coating applying a normal load of 200N, thereby causing layer damage to the boundary of the indentation. The results of the test were qualitatively evaluated by comparing the optical microscope images of the crack network and the degree of delamination with an adhesion quality chart which classifies the images into six levels from HF1-HF6 [42]. In this classification, HF1 is featured with only a few minor cracks after indentation which indicates a good bonding while at the other extreme HF6 denotes extensive delamination of the coating and very poor adhesion. Adhesion levels from HF1 to HF4 are typically considered as acceptable coating adhesions for use in commercial applications.

The scratch test was performed by using a spherical Rockwell C diamond indenter (200 µm radius) according to standard testing methods [43]. The indenter was slid over the coating surface and the load increased from 2 to 50 N at a speed of 10 N/mm. The lower critical load, L_{c1}, was defined as the load where the first cracks occurred (representing cohesive failure) and the upper critical load, L_{c2},, was defined as the load associated with the first delamination at the edge of the scratch track (representing adhesive failure). In addition, a load L_{c3} was defined as the load under which the coating was totally removed from the substrate. The scratch tests were repeated for three times in order to obtain reliable results. After scratch testing, the cracking or delamination of the coating was observed using optical microscopy along the scratch track. The cross-section profiles of the DLC coatings at the critical load were measured using an ultimate focus optical microscope operating in the line scanning mode.

3 Experimental results

3.1 Mechanical properties of Ti substrates

The results of optical microscopy and TEM showed that high-pressure torsion processing significantly refined the grain size of pure Ti from ~8.6 μm in the as-received state to ~130 nm after high-pressure torsion processing. Due to this grain refinement, the microhardness of pure Ti increased from an initial value of ~1.82 GPa in the coarse-grained state to ~3.05 GPa after high-pressure torsion processing. This latter value for the ultrafine-grained pure Ti is comparable with the hardness of 3.09 GPa for the Ti-6Al-4V alloy used in this study [5].

The tensile testing demonstrated that the ultimate tensile strength (UTS) of Ti increased from ~660 MPa in the coarse-grained state to ~940 MPa after high-pressure torsion with some associated reduction in ductility [19]. This high strength and reasonable ductility of ultrafine-grained pure Ti is compatible with the Ti-6Al-4V alloy where the UTS is ~980 MPa and the elongation to failure is ~14%.

3.2 Coating characterisation

Table 2 shows the zirconium content, the hardness and the values of the Young modulus of the deposited coatings. It should be noted that the low indentation depth for the indenter (approximately 10% of the coating thickness) made it difficult to ascertain the effect from the substrate material when obtaining these mechanical properties. Details of the coating structure were studied by X-Ray diffraction, Raman spectroscopy and X-Ray photoelectron spectroscopy and these results were reported elsewhere [33, 44]. All of the coatings investigated in this study (with Zr contents of 7-9 at.%) exhibited a nanocomposite structure with very small ZrC nanograins (up to ~2 nm) embedded within an amorphous carbon matrix.

3.3 Adhesion performance of the DLC coatings

Table 3 summaries the adhesion results of DLC coating on all three substrates. The Rockwell C indentation tests showed HF3 and HF4 for all samples with only minor delamination and micro-cracking observed around the indentation marks, thereby demonstrating an acceptable adhesion for all tested coatings. The scratch test results showed that the DLC coatings with UFG Ti and Ti-6Al-4V substrates had similar critical loads and these loads were much higher than with the coarse-grained Ti as substrates. Thus, the UFG Ti and Ti-6Al-4V substrates provided better support with their higher hardness and this produced a higher critical load of the DLC coating. These results demonstrate again the important role of substrates for the adhesion of thin DLC coatings.

Optical images of the Rockwell indentations are shown in Fig. 1. It can be seen that the load of 200 N led to radial plastic deformation of the coating which caused circumferential cracking of the film outside the indentation area. Through-thickness cracks were observed on all coatings which may be related to the elastic-plastic boundary of the substrates. The indentation marks had a diameter of ~380 μm on the DLC/coarse-grained Ti samples which would cause more deformation at the edge and more delamination compared to the DLC/ultrafine-grained Ti and DLC/Ti-6Al-4V samples. This effect was mainly caused by the different hardness of the Ti substrates. Furthermore, the doping of H content led to a decrease of the adhesion strength because all the indents of the DLC:H-7Zr coating showed a higher delamination than DLC-7Zr. It is obvious that the DLC-9Zr coatings with higher Zr content presented the best adhesion behaviour with only small cracks and minor coating delamination. Therefore, it may be possible to further enhance the coating adhesion by increasing the zirconium content. A more comprehensive study of the adhesion of DLC coatings with different Zr content is given elsewhere [44].

The scratch test results matched well with observation from the Rockwell indentations. Figure 2 shows the scratch tracks of the DLC-7Zr coating on the Ti substrates with increasing loads from 2 to 50 N. Generally, the plastic deformation of the Ti substrates was the main cause for the coating failure. As the diamond stylus was sliding with increasing normal load on the coating surface, the coating followed the deformation of the Ti substrate. The tensile stress both inside the coating and at the interface led to cracking and delamination of the coatings. As shown in Fig .2 (a), the DLC-7Zr coating on coarse-grained Ti failed at an early stage during the scratch test and the indenter caused extensive deformation of the substrate. On the other hand, the DLC-7Zr coatings deposited on ultrafine-grained Ti and Ti-6Al-4V failed at a higher load and the adhesion of the films deposited on both substrates was almost identical (Fig.2 (b) and (c)). The cross-section of the scratch tracks where the substrate was revealed in the scratch track (see the short vertical lines in Fig. 2 (a), (b) and (c)) was measured using an ultimate focus optical microscope. Although the coating was deposited onto different substrates, these measurements showed that it always failed when the scratch track was approximately 7 μm deep and 130 μm wide as illustrated in Fig. 3.

4 Discussion

In this study, a grade 2 pure Ti was processed using high-pressure torsion to achieve significant grain refinement and then DLC coatings were successfully deposited on the different Ti substrates and their scratch behaviour was studied. In terms of future bio-medical applications, the results provide a clear demonstration that it is possible to replace the conventional Ti-6Al-4V alloy with ultrafine-grained pure Ti having preferable mechanical properties which may be achieved through high-pressure torsion processing.

Various coating technologies are now available to provide wear resistance for bio-implants. Technologies such as plasma electrolytic oxidation (PEO) and internal oxidation (IO) have been used extensively to process Ti-6Al-4V and other bio-metals but these methods often involve a high processing temperature which may lead to recrystallization of ultrafine-grained structures [45, 46]. When ultrafine-grained materials are chosen as the substrates, the post processing temperature must not exceed the recrystallization temperature in order to restrict any grain growth of the ultrafine-grained structures. Moreover, the oxidation layers produced through these methods are often very rough and this will entail additional polishing before their use in implants. Thus, PVD methods are regarded as one of the best choices for surface modifying ultrafine-grained materials.

A good adhesion between the thin coating and the substrate is essential for the coating/substrate system. The interposition of a gradient layer (Ti/TiN/TiCN) improves the interface shear strength and the load bearing capacity of the coating [28]. It was observed in this study that, when using ultrafine-grained Ti as the substrate, the load bearing capacity of DLC coatings was improved extensively compared to those with coarse-grained Ti as substrates. A similar trend was observed also on TiN thin coatings on different Ti substrates [19]. The TiN on ultrafine-grained Ti also had a higher critical failure load as it prevented the thin coating from undergoing deformation. Figure 4 shows the critical load of the DLC coatings and TiN coating on Ti substrates plotted against the hardness of the substrate. The trend is clear because a harder substrate after high-pressure torsion leads to a higher critical load for the coatings. Therefore, on one hand it is very important to explore better coating parameters such as new interlayer designs and coating compositions in order to achieve a good performance of the coatings. On the other hand, it is also very important to enhance the properties of substrates through surface hardening or grain refinement (i.e. increase the H/E ratio) and thereby give a better support to the thin coatings.

The results from this research showed that the DLC coating failures occurred at the same depth and width of penetration for all three substrates, as is clearly observed in Fig 3. As the UFG Ti and Ti-6Al-4V had very similar hardness, therefore, the datum points were very close to each other. As shown in Fig 3, the critical load of all coatings increased with increasing hardness of the substrates. A similar trend was also observed on various TiN coated substrates including stainless steel, high speed steel and WC [47]. An explanation was given by assuming the TiN coating adjusted to the elastic–plastic deformation of the substrates, therefore the coating underwent a cohesive–adhesive failure that leads to film delamination. A critical indentation width of 60 μm was observed in that study, where the coating failed whenever it was bent to this width regardless of the substrate material.

By simplifying the coating-substrate system as a two-layer composite, the overall hardness of the coating-substrate system may be represented by the following relationship according to the Burnett-Rickerby model which is based on a volume law of mixtures [47-50]:

$$H_{C,S} = \frac{V_C}{V_{total}} H_C + \frac{\chi^3 V_S}{V_{total}} H_S \tag{2}$$

where $H_{C,S}$ is the apparent hardness of the coating-substrate system, H_S is the hardness of the substrate, H_C is the hardness of the coating, χ is a factor by which the plastic zone changes, and the V_C, V_S and V_{total} are the deformation volumes of the coating, substrate and total deformation volume, respectively.

The volumes of the deformation zones are expressed by the following equations:

$$V_C \approx \pi R_C^2 t \tag{3}$$

$$V_S \approx \chi^3 \frac{2}{3} \pi R_S^3 \tag{4}$$

where R_C and R_S are the radius of deformation zone of coating and substrate. The factor, χ was determined via fitting experimental results by Burnett and Rickerby [48] and addressed as:

$$\chi = \left(\frac{E_C H_S}{E_S H_C} \right)^{1/2} \tag{5}$$

where E_C and H_C are the Young's Modulus and hardness of the coating, and E_S and H_S are the Young's Modulus and hardness of the substrate. R_C and R_S can be obtained through the equation:

$$R = r \left(\frac{E}{H} \right)^{1/2} \tag{6}$$

where r is the geometrical length of the indentation volume.

As observed in Fig 3, the indentation depths of all samples were only around 7 μm, and this depth was obtained after the diamond indenter was removed. In this case, the measured indentation depth was underestimated due to the elastic recovery of materials. Therefore, it is more accurate to recalculate the indentation depth using the measured indentation width considering the sphere shape of the indenter, according to the equation:

$$r = \left[\pi \left(R_{ind}^{2} - \frac{W^{2}}{4} \right) \left(R_{ind} - \frac{\sqrt{R_{ind}^{2} - \frac{W^{2}}{4}}}{3} \right) \right]^{1/3} \tag{7}$$

where R_{ind} is the radius of diamond indenter and W is the track width at the critical load point.

Therefore, the overall hardness of this coating-substrate is achieved by rewriting equations (2-6):

$$H_{C,S} = \frac{E_C t + \frac{2}{3} r H_S \left(\frac{E_C}{H_C} \right)^{3/2}}{\frac{E_C}{H_C} t + \frac{2}{3} r \left(\frac{E_C}{H_C} \right)^{3/2}} \tag{8}$$

During the scratch testing, the indenter was travelling with an increasing normal load and it was always the front half of the spherical cap in the coating-substrate system. Therefore, the critical load, L_{C3}, is expressed as:

$$L_{C3} = H_{C,S} \pi R_{ind} \sqrt{R_{ind}^{2} - \frac{W^{2}}{4}} \tag{9}$$

Thus, equations (8) and (9) clearly emphasise the effect of substrate strength on the scratch behaviour of thin coatings. It further explains that the DLC coatings, with thicknesses around 1 μm, often exhibit high critical loads with hard materials as substrates, such as more than 100 N on Si or glass [51].

The track width of each sample is listed in Table 3 and this can be applied to equations (8) and (9). The comparison between experimental results and the Burnett-Rickerby model is plotted in Fig 5. It worth noting that as the interlayers had varying compositions and properties and were much thinner than the coatings, thus this analysis simply neglects the properties of the interlayers although in practice the interlayer is important in improving the bonding. This may lead to an underestimation of the model. Moreover, errors may also be introduced due to the ridges formed at the edge of the scratch tracks which made it difficult to measure the track widths.

In this study, the strength and hardness of pure Ti was successfully improved by high-pressure torsion processing. Firstly, this improves the mechanical durability of pure Ti as the main body of bio-implants when they suffer fatigue and shear loadings. Secondly, ultrafine-grained pure Ti is a good substrate for thin coatings and provides improved load bearing capacity of the coating. Therefore, with good strength, fatigue life, excellent bio-compatibility and no toxic release tendency of ultrafine-grained pure Ti, and with good wear resistance and an extremely low coefficient of friction of the DLC coatings, the DLC/ultrafine-grained Ti system appears to be an exceptionally strong candidate material for future bio-implant applications.

Conclusions

The adhesion behaviour and scratch resistance of three diamond-like carbon coatings deposited on grade 2 pure Ti substrates before and after high-pressure torsion processing were investigated and a comparison was made with a Ti-6Al-4Vsubstrate. The following conclusions are reached:

1. DLC coatings with a gradient TiN/TiCN interlayer show good adhesion on Ti substrates.
2. Hydrogen-free DLC-Zr coatings have better adhesion than hydrogen-doped DLC-Zr coatings, and increase of the percentage of Zr increases the adhesion.
3. The effect of substrate on the performance of the DLC coating under high load was highlighted, showing that coatings with ultrafine-grained pure Ti and Ti-6Al-4V substrates have similar scratch and indentation behaviour. Both are significantly better than the results obtained with coarse-grained Ti substrates.

Acknowledgements

The authors are grateful for support from the University of Southampton together with a scholarship from the China Scholarship Council (CTW). This work was partially supported by EPSRC under Grant No. EP/D00313X/1 and by the National Science Foundation of the United States under Grant No. DMR-1160966 (TGL). The authors also acknowledge FCT-Fundação para a Ciência e a Tecnologia (QREN-POPH) for funding support under Grant SFRH/BD/75071/2010 which was co-funded by FSE and MSTES.

References

[1] M. Geetha, A.K. Singh, R. Asokamani, A.K. Gogia, Ti based biomaterials, the ultimate choice for orthopaedic implants - A review, Prog. Mater. Sci. 54 (2009) 397-425.

[2] S.S. Leopold, Numbers for breakfast: summary of hip arthroplasty outcomes from the national joint registry for England and wales 8th annual report (2011), J. Bone. Joint. Surg. Am. 93 (2011) 1-3.

[3] Y. Li, C. Wong, J. Xiong, P. Hodgson, C. Wen, Cytotoxicity of Titanium and Titanium Alloying Elements, J. Dent. Res. 89 (2010) 493-497.

[4] S. Makihira, Y. Mine, H. Nikawa, T. Shuto, S. Iwata, R. Hosokawa, K. Kamoi, S. Okazaki, Y. Yamaguchi, Titanium ion induces necrosis and sensitivity to lipopolysaccharide in gingival epithelial-like cells, Toxicol. In. Vitro. 24 (2010) 1905-1910.

[5] C.T. Wang, N. Gao, M.G. Gee, R.J.K. Wood, T.G. Langdon, Effect of grain size on the micro-tribological behavior of pure titanium processed by high-pressure torsion, Wear. 280 (2012) 28-35.

[6] V.L. Sordi, M. Ferrante, M. Kawasaki, T.G. Langdon, Microstructure and tensile strength of grade 2 titanium processed by equal-channel angular pressing and by rolling, J. Mater. Sci. 47 (2012) 7870-7876.

[7] R.Z. Valiev, T.G. Langdon, Principles of equal-channel angular pressing as a processing tool for grain refinement, Prog. Mater. Sci. 51 (2006) 881-981.

[8] A.P. Zhilyaev, T.G. Langdon, Using high-pressure torsion for metal processing: Fundamentals and applications, Prog. Mater. Sci. 53 (2008) 893-979.

[9] R.Z. Valiev, I.V. Alexandrov, Y.T. Zhu, T.C. Lowe, Paradox of strength and ductility in metals processed by severe plastic deformation, J. Mater. Res. 17 (2002) 5-8.

[10] M. Kautz, H.W. Höppel, C. Xu, M. Murashkin, T.G. Langdon, R.Z. Valiev, H. Mughrabi, An overview: fatigue behaviour of ultrafine-grained metals and alloys, Intl. J. Fatigue 28 (2006) 1001-1010.

[11] I.P. Semenova, R.Z. Valiev, E.B. Yakushina, G.H. Salimgareeva, T.C. Lowe, Strength and fatigue properties enhancement in ultrafine-grained Ti produced by severe plastic deformation, J. Mater.Sci. 43 (2008) 7354-7359.

[12] C.T. Wang, N. Gao, R.J.K. Wood, T.G. Langdon, Wear behavior of an aluminum alloy processed by equal-channel angular pressing, J. Mater. Sci. 46 (2011) 123-130.

[13] N. Gao, C.T. Wang, R.J.K. Wood, T.G. Langdon, Tribological properties of ultrafine-grained materials processed by severe plastic deformation, J. Mater. Sci. 47 (2012) 4779-4797.

[14] X. Zhao, W. Fu, X. Yang, T.G. Langdon, Microstructure and properties of pure titanium processed by equal-channel angular pressing at room temperature, Scr. Mater. 59 (2008) 542-545.

[15] X. Zhao, X. Yang, C. Wang, X. Wang, T.G. Langdon, The processing of pure

titanium through multiple passes of ECAP at room temperature, Mater. Sci. Eng. A527 (2010) 6335-6339.

[16] I. Sabirov, R.Z. Valiev, I.P. Semenova, R. Pippan, Effect of Equal Channel Angular Pressing on the Fracture Behavior of Commercially Pure Titanium, Metall. Mater. Trans. A. 41A (2010) 727-733.

[17] Y. Zhang, R.B. Figueiredo, S.N. Alhajeri, J.T. Wang, N. Gao, T.G. Langdon, Structure and mechanical properties of commercial purity titanium processed by ECAP at room temperature, Mater. Sci. Eng. A. 528 (2011) 7708-7714.

[18] P. La, J. Ma, Y.T. Zhu, J. Yang, W. Liu, Q. Xue, R.Z. Valiev, Dry-sliding tribological properties of ultrafine-grained Ti prepared by severe plastic deformation, Acta. Mater. 53 (2005) 5167-5173.

[19] C.T. Wang, N. Gao, M.G. Gee, R.J. Wood, T.G. Langdon, Processing of an ultrafine-grained titanium by high-pressure torsion: an evaluation of the wear properties with and without a TiN coating, J. Mech. Behav. Biomed. Mater. 17 (2013) 166-175.

[20] A.V. Byeli, V.A. Kukareko, A.G. Kononov, Titanium and zirconium based alloys modified by intensive plastic deformation and nitrogen ion implantation for biocompatible implants, J. Mech. Behav. Biomed. Mater. 6 (2012) 89-94.

[21] H. Dong, W. Shi, T. Bell, Potential of improving tribological performance of UHMWPE by engineering the Ti6Al4V counterfaces, Wear. 225–229 (1999) 146-153.

[22] Z.X. Zhang, H. Dong, T. Bell, The load bearing capacity of hydrogen-free Cr-DLC coatings on deep-case oxygen hardened Ti6Al4V, Surf. Coat. Technol.200 (2006) 5237-5244.

[23] R.Z. Valiev, A.V. Sergueeva, A.K. Mukherjee, The effect of annealing on tensile deformation behavior of nanostructured SPD titanium, Scr. Mater. 49 (2003) 669-674.

[24] V.M. Tiainen, Amorphous carbon as a bio-mechanical coating-mechanical properties and biological applications, Diam. Relat. Mater. 10 (2001) 153-160.

[25] T.J. Joyce, Examination of failed ex vivo metal-on-metal metatarsophalangeal prosthesis and comparison with theoretically determined lubrication regimes, Wear. 263 (2007) 1050-1054.

[26] C.V. Falub, U. Mueller, G. Thorwarth, M. Parlinska-Wojtan, C. Voisard, R. Hauert, In vitro studies of the adhesion of diamond-like carbon thin films on CoCrMo biomedical implant alloy, Acta. Mater. 59 (2011) 4678-4689.

[27] R. Hauert, G. Thorwarth, U. Mueller, M. Stiefel, C.V. Falub, K. Thorwarth, T.J. Joyce, Analysis of the in-vivo failure of the adhesive interlayer for a DLC coated articulating metatarsophalangeal joint, Diam. Relat. Mater. 25 (2012) 34-39.

[28] J. Chen, G.A. Bell, B.D. Beake, H. Dong, Low Temperature Nano-Tribological Study on a Functionally Graded Tribological Coating Using Nanoscratch Tests, Tribol. Lett. 43 (2011) 351-360.

[29] A. Pardo, C. Gomez-Aleixandre, J.O. Orwa, A. Cimmino, S. Prawer, Modification of characteristics of diamond-like carbon thin films by low chromium content addition, Diam. Relat. Mater. 26 (2012) 39-44.

[30] F. Zhao, H. Li, L. Ji, Y. Wang, H. Zhou, J. Chen, Ti-DLC films with superior friction performance, Diam. Relat. Mater. 19 (2010) 342-349.

[31] A. Czyzniewski, Optimising deposition parameters of W-DLC coatings for tool materials of high speed steel and cemented carbide, Vacuum. 86 (2012) 2140-2147.

[32] D.B.N. Lee, M. Roberts, C.G. Bluchel, R.A. Odell, Zirconium: Biomedical and Nephrological Applications, Asaio J. 56 (2010) 550-556.

[33] A. Escudeiro, T. Polcar, A. Cavaleiro, a-C(:H) and a-C(:H)_Zr coatings deposited on biomedical Ti-based substrates: Tribological properties, Thin. Solid. Films. (2012) In Press.

[34] P. Kumar, P. Dilli Badu, L. Moham, C. Anandan, V. Grips, Wear and Corrosion Resistance of Zr doped DLC on Ti-13Zr-13Nb Biomedical Alloy, J. Mater. Eng. Perform. (2012) In Press.

[35] R.Z. Valiev, Yu.V. Ivanisenko, E.F. Rauch, B. Baudelet, Structure and deformation behaviour of Armco iron subjected to severe plastic deformation, Acta Mater. 44 (1996) 4705-4712.

[36] R.B. Figueiredo, P.R. Cetlin, T.G. Langdon, Using finite element modeling to examine flow processes in quasi-constrained high-pressure torsion, Mater. Sci. Eng. A528 (2011) 8198-8204.

[37] R.B. Figueiredo, P.H.R. Pereira, M.T.P. Aguilar, P.R. Cetlin, T.G. Langdon, Using finite element modeling to examine the temperature distribution in quasi-constrained high-pressure torsion, Acta Mater. 60 (2012) 3190-3198.

[38] A.P. Zhilyaev, G.V. Nurislamova, B.K. Kim, M.D. Baró, J.A. Szpunar, T.G. Langdon, Experimental parameters influencing grain refinement and microstructural evolution during high-pressure torsion, Acta. Mater. 51 (2003) 753-765.

[39] M. Kawasaki, T.G. Langdon, The significance of strain reversals during processing by high-pressure torsion, Mater. Sci. Eng. A498 (2008) 341-348.

[40] C.T. Wang, N. Gao, R.J.K. Wood, T.G. Langdon, Wear Behaviour of Al-1050 Alloy Processed by Severe Plastic Deformation, Mater. Sci. Forum. 667-669 (2011) 1101-1106.

[41] W.C. Oliver, G.M. Pharr, An improved technique for determining hardness and elastic-modulus using load and displacement sensing indentation experiments, J. Mater. Res. 7 (1992) 1564-1583.

[42] N. Vidakis, A. Antoniadis, N. Bilalis, The VDI 3198 indentation test evaluation of a reliable qualitative control for layered compounds, J. Mater. Process. Technol. 143 (2003) 481-485.

[43] J. Stallard, S. Poulat, D.G. Teer, The study of the adhesion of a TiN coating on steel and titanium alloy substrates using a multi-mode scratch tester, Tribol. Int. 39 (2006) 159-166.

[44] A. Escudeiro, T. Polcar, A. Cavaleiro, DLC(H) doped with Zr coatings for orthopaedics applications: Adhesion properties, SVC Spring 2013 Bulletin.

[45] J.M. Wheeler, C.A. Collier, J.M. Paillard, J.A. Curran, Evaluation of micromechanical behaviour of plasma electrolytic oxidation (PEO) coatings on Ti-6Al-4V, Surf. Coat. Technol. 204 (2010) 3399-3409.

[46] G. Purcek, O. Saray, F. Rubitschek, T. Niendorf, H.J. Maier, I. Karaman, Effect of internal oxidation on wear behavior of ultrafine-grained Nb-Zr, Acta. Mater. 59 (2011) 7683-7694.

[47] A. Rodrigo, P. Perillo, H. Ichimura, On the correlation of substrate microhardness with the critical load of scratch adherence for hard coatings, Surf. Coat. Technol.124 (2000) 87–92.

[48] P.J. Burnett, D.S. Rickerby, The mechanical properties of wear resistant coatings.1.modelling of hardness behaviour, Thin Solid Films 148 (1987) 41-50.

[49] P.J. Burnett, D.S. Rickerby, The relationship between hardness and scratch adhesion, Thin Solid Films 154 (1987) 403-416.

[50] A. Rodrigo, H. Ichimura, Analytical correlation of hardness and scratch sdhesion for hard films, Surf. Coat. Technol.148 (2001) 8-17.

[51] Y. Huang, Q. Wang, M. Wang, Z. Fei, M. Li, Characterization and analysis of DLC films with different thickness deposited by RF magnetron PECVD, Rare. Metals. 31 (2012) 198-203.

Table 1 Deposition parameters of DLC-XZr and DLC:H-XZr coatings

Parameters	DLC-XZr	DLC:H-XZr
Reactive gas flow (%)	---	5
Ar flow (%)	45	40
Base pressure (Pa)	$1.5x10^{-3}$	
Work Pressure (Pa)	0.4	
Substrate bias (V)	-50	
Graphite doped target (W/mm^2)	0.075	

Table 2 Summary of coatings chemical composition and mechanical properties.

System	Zr content (at.%)	Hardness (GPa)	E(GPa)
DLC_7Zr	7±1	11±2	120±3
DLC:H_7Zr	8±1	13±1	117±4
DLC_9Zr	10±1	12±2	131±3

Table 3 Summary of adhesion results

Substrate	Coating	Rockwell C		Scratch			
		Ø (μm)	adhesion	Lc1 (N)	Lc2 (N)	Lc3 (N)	Track width at Lc3 (μm)
CG Ti	DLC_7Zr	375	HF3	7±2	8±1	13±2	149.7
	DLC:H_7Zr	391	HF4	5±1	7±2	13±1	130.1
	DLC_9Zr	384	HF4	7±1	9±1	15±1	130.7
UFG Ti	DLC_7Zr	282	HF3	8±1	12±1	22±2	113.3
	DLC:H_7Zr	286	HF3	7±2	10±1	20±1	120.9
	DLC_9Zr	287	HF3	10±2	14±1	24±1	123.8
Ti-6Al-4V	DLC_7Zr	277	HF3	9±2	11±1	23±2	139.7
	DLC:H_7Zr	274	HF4	5±1	10±2	19±2	132.1
	DLC_9Zr	282	HF3	11±2	15±1	25±2	126.2

Research Highlights

- Grade 2 pure Ti was processed to grain size of 130 nm by using high-pressure torsion.
- Deposited DLC coatings on ultra-fine grained Ti can improve wear resistance.
- DLC coatings has better load bearing capacity with ultra-fine grained Ti as substrate.
- Ultra-fine grained Ti plus DLC coating provides an important material for bio-implants.

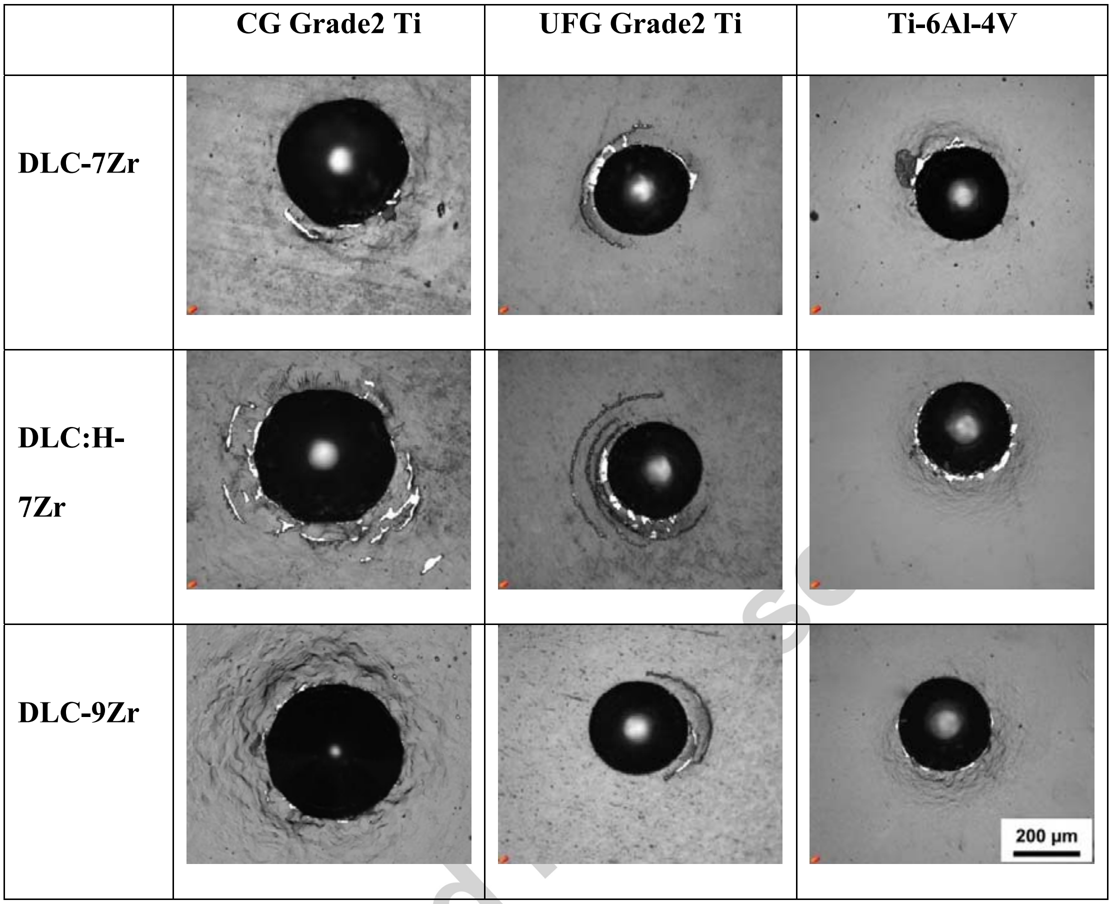

Figure 1 Rockwell indentation of DLC on different Ti substrates.

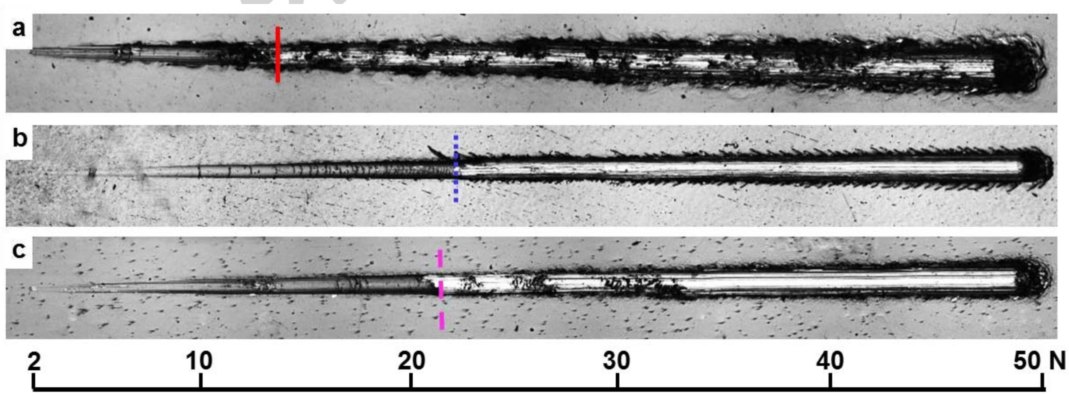

Fig.2 Scratch tracks of DLC-7Zr coatings on (a) coarse-grained Ti, (b) ultrafine-grained Ti, (c) Ti-6Al-4V substrates.

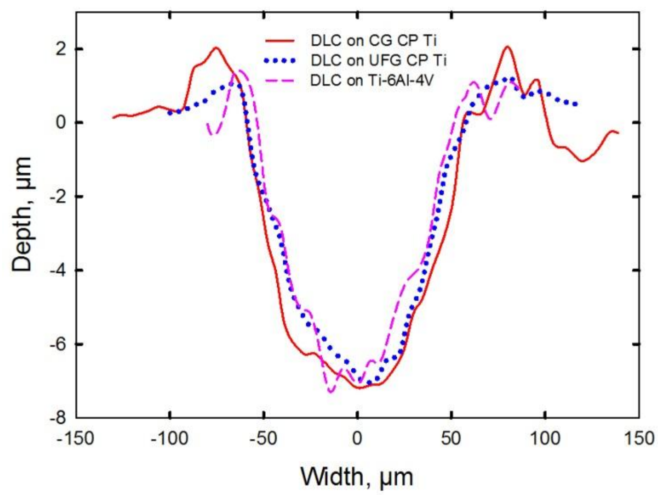

Fig. 3 Cross-section of the scratch tracks in the positions indicated in Fig. 2.

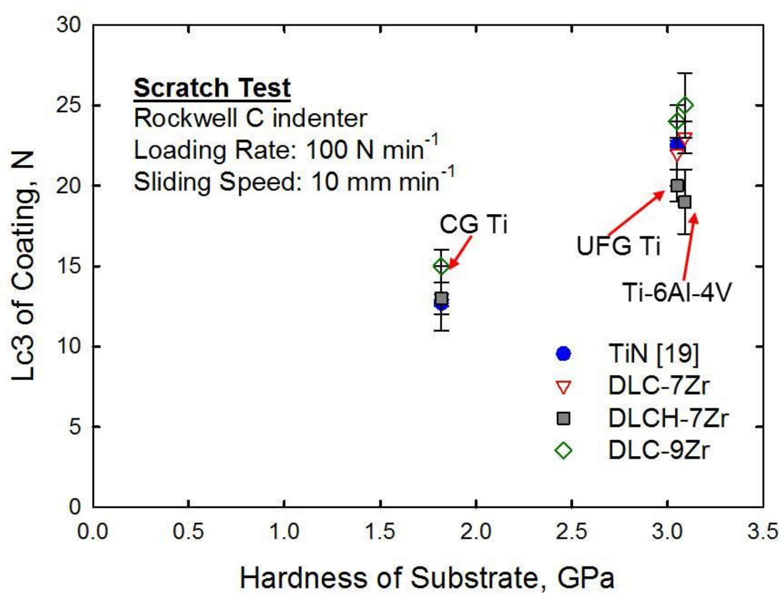

Fig.4 Critical load of coatings versus the hardness of substrates.

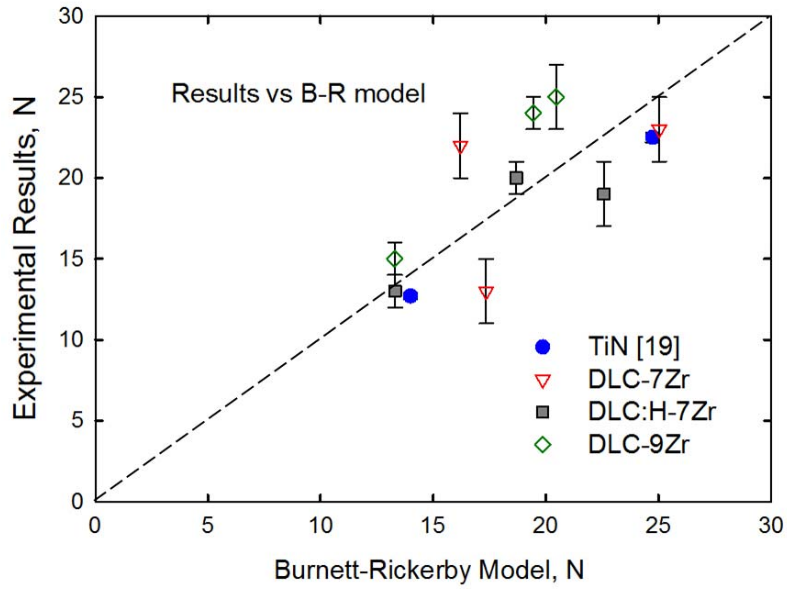

Fig.5 Comparison of critical load between experimental results and calculation from Burnett-Rickerby model.